Development of multi-model ensemble for projection of extreme rainfall events in Peninsular Malaysia

Muhammad Noor, Tarmizi Ismail, Shamsuddin Shahid, Mohamed Salem Nashwan and Shahid Ullah

ABSTRACT

Possible changes in rainfall extremes in Peninsular Malaysia were assessed in this study using an ensemble of four GCMs of CMIP5. The performance of four bias correction methods was compared, and the most suitable method was used for downscaling of GCM simulated daily rainfall to the spatial resolution (0.25°) of APHRODITE rainfall. The multi-model ensemble (MME) mean of the downscaled rainfall was developed using a random forest regression algorithm. The MME projected rainfall for four RCPs were compared with APHRODITE rainfall for the base year (1961–2005) to assess the annual and seasonal changes in eight extreme rainfall indices. The results showed power transformation as the most suitable bias correction method. The maximum changes in most of the annual and seasonal extreme rainfall indices were observed for RCP8.5 in the last part of this century. The maximum increase was observed for 1-day and 5 consecutive days' rainfall amount for RCP4.5. Spatial distribution of the changes revealed higher increase of the extremes in the northeast region where rainfall extremes are already very high. The increase in rainfall extremes would increase the possibility of frequent hydrological disasters in Peninsular Malaysia.

Key words | climate change, downscaling, extremes, GCMs, Malaysia, MME

Muhammad Noor (corresponding author)
Tarmizi Ismail
Shamsuddin Shahid
Mohamed Salem Nashwan
Faculty of Engineering,
Universiti Teknologi Malaysia (UTM),
81310 Skudai, Johor,
Malaysia
E-mail: *mnkakar@gmail.com*

Mohamed Salem Nashwan
College of Engineering and Technology,
Arab Academy for Science,
Technology and Maritime Transport (AASTMT),
Cairo,
Egypt

Shahid Ullah
The Agriculture and Cooperative Department,
Government of Balochistan,
Quetta,
Pakistan

INTRODUCTION

Changes in both magnitude and variability of rainfall have been reported in different regions of the world due to global warming induced by climate change (IPCC 2013). Small changes in the mean and variance due to climate change can produce relatively large changes in the probability of extreme events (Shahid *et al.* 2016; Nashwan *et al.* 2019d). Therefore, increases in rainfall extremes have been observed in many countries (Nashwan *et al.* 2019c; Shiru *et al.* 2019). Assessment of such changes is of importance for developing adaptation strategies to reduce the risks of precipitation extremes. A complete analysis of climate events requires an analysis of both their spatial and temporal extent (Shahid 2009, 2010). Global climate models are the main tools used by the scientific community to reproduce the current climate and project future changes of extreme precipitation events. To facilitate research on climate extremes, the Joint World Meteorological Organization (WMO) Expert Team on Climate Change Detection and Indices (ETCCDI) has defined a set of climate change indices focusing on extremes that can be described from daily temperature and precipitation across different parts of the world (Zhang *et al.* 2011). These indices have been widely used in detection, attribution and projection of changes in climate extremes (Alexander *et al.* 2006; Min *et al.* 2011; Donat *et al.* 2013; Sillmann *et al.* 2013a, 2013b; Wen *et al.* 2013; Zhou *et al.* 2014; Nashwan & Shahid 2019a, Nashwan *et al.* 2019b). Sillmann *et al.* (2013a) compared ETCCDI indices computed from observations and model simulations by the Coupled Model Intercomparison Project phase 5 (CMIP5) and found that CMIP5 models are generally able

doi: 10.2166/nh.2019.097

to reproduce the historical trend patterns of these extreme climate indices.

One of the major concerns in the simulation of observed climate at the local scale is the reliability of GCMs (Rupp *et al.* 2013). Due to their coarse spatial resolution and other uncertainties, the projections of GCMs cannot be used at the local scale for projection spatial distribution and extreme precipitation indices (Pour *et al.* 2014; Ahmed *et al.* 2015a; Nashwan *et al.* 2019a). A technique known as downscaling is used for bridging the gap between the higher GCMs resolution and local climate processes. There are two major types of downscaling techniques, statistical downscaling and dynamical downscaling. Due to low computational cost, statistical downscaling methods are preferred over dynamic downscaling (Mpelasoka & Chiew 2009; Lin *et al.* 2017; Salman *et al.* 2018). Model output statistics (MOS) and perfect prognosis (PP) are the two main types of statistical downscaling techniques (Maraun *et al.* 2010; Pour *et al.* 2018). MOS is often preferred due to its capacity to correct model-inherent errors and biases in GCM simulation (Eden & Widmann 2014; Pour *et al.* 2018; Chen *et al.* 2019). In MOS approach, the bias in historical simulation of GCMs are corrected based on observation (Noor *et al.* 2018). The bias correction parameters are then used to correct the bias in GCM projections for future scenarios (Widmann *et al.* 2003; Turco *et al.* 2017).

The performance of a MOS model depends on the bias correction method used (Guo *et al.* 2019). Considering the complex relationship between GCM simulations and observations, a large number of bias correction methods have been proposed and successfully applied (Gudmundsson *et al.* 2012; Sachindra *et al.* 2014; You *et al.* 2018). It has been reported that the performance of different bias correction methods depends on the nature of climate data (Ahmed *et al.* 2015b, 2018). Therefore, it is important to select the most suitable method through the evaluation of various bias correction methods (Ines & Hansen 2006; Sharma *et al.* 2007; Li *et al.* 2010; Gudmundsson *et al.* 2012; You *et al.* 2018).

There is a large number of GCMs developed by various organizations, but the downscaled climate projections of GCMs vary from one another (Scherer & Diffenbaugh 2014; Sa'adi *et al.* 2017). Jiang *et al.* (2012) showed that models have certain abilities to simulate both the spatial distribution and trend of extreme precipitation indices, but because of the limitation of coarse spatial resolution and other uncertainties, the simulation results still show many discrepancies. To reduce the uncertainties associated with the downscaled outputs of GCMs, a multi-model ensemble (MME) approach, in which results of selected GCMs are combined for the projection of climate, is commonly used (Lutz *et al.* 2016; Salman *et al.* 2018; You *et al.* 2018). The MME has been widely applied in the evaluation of models and projection of future climate because it can reduce the uncertainty from individual models and shows superior behaviours compared to any single model (Zhang & Yang 2018).

Various methods are in practice for developing MME (Ahmed *et al.* 2019). Commonly, mean of the selected GCMs is used to develop MME (Pierce *et al.* 2009). This approach can be justified for global-scale climate assessment; however, it cannot be used at regional scale as the good performing GCMs are given the same weightage as the bad performing GCMs in such an approach (Gleckler *et al.* 2008; Reichler & Kim 2008). The regression-based MME is also very popular due to its capability to keep the variance in the mean (Steinschneider *et al.* 2015; Ishizaki *et al.* 2017; Salman *et al.* 2018). Data mining-based regression has received attention in recent years due to its ability to capture the nonlinear relationships between the independent and target variable (Sa'adi *et al.* 2017). Ahmed *et al.* (2018) used a random forest (RF), a machine learning algorithm, to develop MME of four CMIP5 GCMs and reported that RF can be efficiently used for developing MME. Salman *et al.* (2018) also developed a single ensemble projection from outputs of different GCMs by using RF regression technique. The studies indicated that a MME developed from a suitable set of GCMs using RF method can efficiently be used for reducing the associated uncertainties in climate projections (Nashwan & Shahid 2019b).

The global change in climate is also affecting Malaysia, especially in terms of the hydrologic cycle. The mean temperature in Malaysia has increased in the range of 0.6 °C to 1.2 °C per 50 years (Paterson *et al.* 2015). The increase in temperature and variations in rainfall patterns can severely affect the hydrological regimes as well as the quantity of runoff in Malaysia (Sa'adi *et al.* 2017; Noor *et al.* 2018). For developing an effective policy to adapt to these climate

variations, it is necessary to analyse and understand the present and possible future climate changes (Batisani & Yarnal 2010; Shahid *et al.* 2016; Wang *et al.* 2014, 2017). One of the ways to reduce the vulnerability is to quantify and adapt to these impacts expected to be caused by possible climate change.

The major objective of this work is to use an ensemble of four CMIP5 GCMs of the Fifth Assessment Report (AR5) of IPCC to assess the possible spatial variation in rainfall extremes in Peninsular Malaysia under changing climate scenarios. Due to unavailability of quality and long-term rainfall observation from the network of rain gauge stations in Peninsular Malaysia, the GCM simulated daily rainfall was downscaled based on Asian Precipitation-Highly Resolved Observational Data Integration Towards Evaluation of Water Resources (APHRODITE) rainfall. An RF nonlinear regression algorithm was used to develop an ensemble of the projected rainfall for the period of 2010–2099 separately for all four RCPs. The spatial variation of projected rainfall for three periods, 2010–2039, 2040–2069 and 2070–2099, was finally computed for each RCP. The projected changes in the annual and seasonal indices are summarized using box-and-whisker plots. It is expected that the study would help to understand the possible changes in rainfall extremes in Peninsular Malaysia, resulting in taking policy measures to adapt with the changing pattern of climate.

STUDY AREA AND DATA

Study area

Peninsular Malaysia, situated in the tropics between latitude 1.20° and 6.40° north, and longitude 99.35° and 104.20° east (Figure 1) covers an area of 130,598 km^2. It has a hot and humid climate which is influenced by monsoon winds, mountainous topography and complex land–sea interactions (Mayowa *et al.* 2015; Nashwan *et al.* 2018a; Muhammad *et al.* 2019). It has two rainy seasons, the northeast (NE) monsoon (November to March) and the southwest (SW) monsoon (May to September) with annual rainfall ranges between 2,000 and 4,000 mm and 150–200 wet days (Shahid *et al.* 2017; Nashwan *et al.* 2018b).

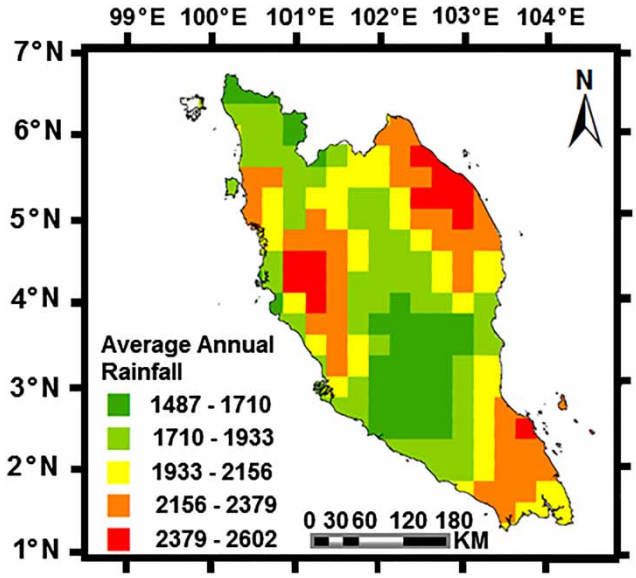

Figure 1 | A map of Peninsular Malaysia showing the average annual rainfall estimated using APHRODITE v.1 dataset for the period 1961–2005.

Data and sources

The gridded daily rainfall data of APHRODITE v.1 having a spatial resolution of 0.25° × 0.25° for the period 1961–2005 was used in the current study to represent historical observations. APHRODITE has been developed using rain-gauge data of the Global Telecommunication System reports and collections of national-level gauge networks. A number of studies have recognized APHRODITE as the representative rainfall data for Peninsular Malaysia (Ou *et al.* 2013; Chen *et al.* 2018b; Khan *et al.* 2018, 2019). Ou *et al.* (2013) reported that estimation of extreme rainfall indices using APHRODITE is very similar to that obtained from station-based data. Khan *et al.* (2018) suggested that APHRODITE can be efficiently used for the projection of rainfall. In another study, Khan *et al.* (2019) found APHRODITE to be suitable for assessing the spatial patterns of the trends in rainfall extremes of Peninsular Malaysia. APHRODITE has been developed using ground observations and, therefore, used as reference data in many studies (Chen *et al.* 2018a). Therefore, APHRODITE was used in the present study to represent historical observations of rainfall.

The gridded daily rainfall of GCMs, listed in Table 1, was used for the projection of rainfall extremes of Peninsular Malaysia. Noor *et al.* (2019) assessed the performance of

Table 1 | List of the GCMs used in the study for the projection of rainfall extremes in Peninsular Malaysia

Centre	Model	Resolution (lat × long)
Beijing Climate Center China	BCC-CSM1-1(m)	2.8° × 2.8°
National Center for Atmospheric Research USA	CCSM4	0.94° × 1.25°
Commonwealth Scientific and Industrial Research Organization	CSIRO-Mk3-6-0	1.8° × 1.8°
Met Office Hadley Centre UK	HadGEM2-ES	1.25° × 1.875°

23 CMIP5 GCMs based on their ability to replicate APHRODITE daily rainfall in Peninsular Malaysia for the period 1961–2005. They found four GCMs, namely, BCC-CSM1.1(M), CCSM4, CSIRO-Mk3.6.0 and HadGEM2-ES as the most suitable GCMs for the projection of daily rainfall of Peninsular Malaysia. Therefore, those four GCMs are used in the present study for the projection of rainfall extremes in Peninsular Malaysia.

The daily rainfall of the GCMs was obtained from the CMIP5 database of the Fifth Assessment Report of the IPCC (http://www.ipccdata.org/sim/gcm_monthly/AR5/ReferenceArchive.html). They cover the climatic domain of Peninsular Malaysia for the historical (1961–2005) and future projection (2010–2099) under RCP2.6, RCP4.5, RCP6.0 and RCP8.5.

METHODOLOGY

The main objective of this study is to assess the spatial and temporal variation of the projected future seasonal rainfall extremes (Table 2) of Peninsular Malaysia under different climate scenarios using an ensemble of four GCMs (Table 1). The following is an outline of the procedure used in this study.

1. The four GCMs' data (Table 1) were re-gridded spatially to 0.25° × 0.25° to match with APHRODITE spatial resolution.
2. MOS downscaling approach was used for the downscaling of the rainfall of four GCMs for the historical (1961–2005) and future (2010–2099) periods where four different bias correction methods were used.

Table 2 | Rainfall extreme indices used in the study for the assessment of the changes in rainfall extremes in Peninsular Malaysia due to climate change

Index	Definition	Unit
TOTP	Total precipitation in wet days	mm
SDII	Simple daily precipitation intensity	mm
Ex1D	Maximum 1-day precipitation	mm
Ex5D	Maximum consecutive 5-day precipitation	mm
R20	Number of wet days with at least 20 mm of precipitation	days
CDD	Consecutive dry days, the maximum number of consecutive days with less than 1 mm of precipitation	days
CWD	Consecutive wet days, the maximum number of consecutive days with greater than 1 mm of precipitation	days
TRD	Total rainy days	days

3. The output of each bias correction methodology was evaluated using the historical period against APHRODITE data to select the most robust bias correction method to be used in correcting the future period.
4. An ensemble of the downscaled GCMs' projections was generated using RF to reduce the uncertainty in the projection of rainfall.
5. The rainfall extremes (Table 2) were calculated using the ensemble projections of daily rainfall for three different future periods (2010–2039, 2040–2069 and 2070–2099) under different RCP scenarios.
6. The spatial pattern in the temporal changes in the future rainfall extremes during different periods and scenarios based on APHRODITE historical period were plotted and examined.

The methodology for assessing spatial and temporal variation of rainfall extremes is explained step by step as below.

Development of downscaling model

The MOS approach was used for downscaling of the rainfall of four GCMs to APHRODITE resolution. MOS, a statistical downscaling method, is widely employed, using less computational resources but providing as accurate results as the advanced dynamical downscaling methods. In MOS, the four selected GCMs were interpolated to APHRODITE grid

using inverse distance weighting method (IDW). Next, four widely used bias correction methods were used separately to correct the bias in the historical (1961–2005) GCM simulated rainfall based on APHRODITE data. The bias correction methods tested in this study were scaling, power transformation (PT), generalized quantile mapping (Gen QM) and gamma quantile mapping (Gamma QM). The 'downscaleR' package in R was used for the implementation of bias correction methods. The bias correction was done separately for each GCM at each grid point of Peninsular Malaysia. To evaluate the performance of bias correction method, the monthly climatology of mean rainfall and standard deviation of each GCM were calculated and compared with APHRODITE mean and standard deviation. The co-efficient of determination (R^2) and the normalized root mean square error (NRMSE) were calculated for each downscaled

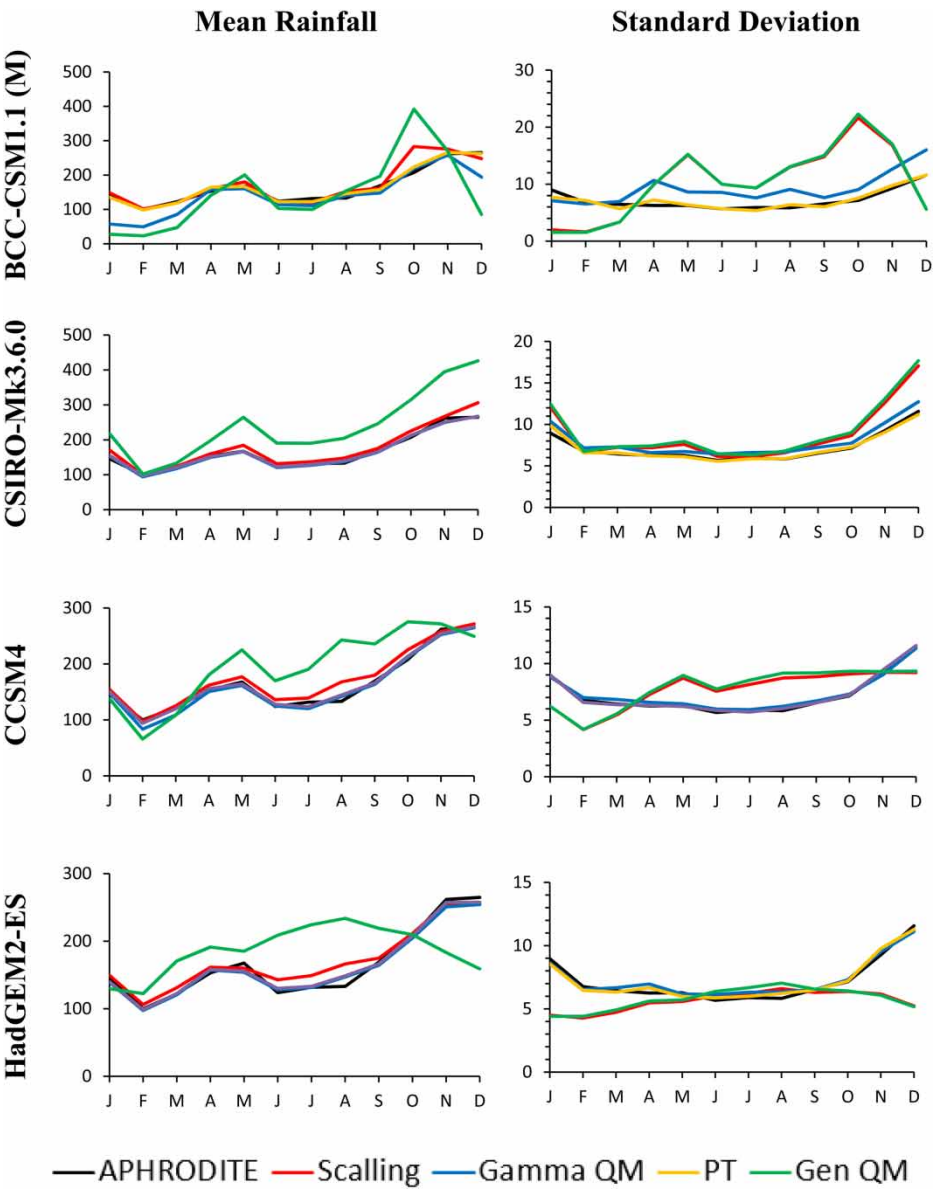

Figure 2 | The mean rainfall (left column) and standard deviation (right column) of BCC-CSM1.1 (M), CSIRO-Mk3.6.0, CCSM4, HadGEM2-ES obtained using different bias correction methods. The Y-axis in the left column represents the mean rainfall in millimetres.

output to select the most suitable bias correction method to be used for the correction of bias in GCM projected rainfall for different scenarios. The following is a brief description of the four bias correction methods used in the present study.

Linear scaling method

The LS method aims to perfectly match the monthly mean of GCM rainfall with APHRODITE rainfall. It operates based on the differences between observed and GCM rainfall. Rainfall is typically corrected with a multiplier as given below:

$$P_{m,d}^{cor} = P_{m,d}^{raw} \times \frac{\mu(P_{obs,m})}{\mu(P_{raw,m})} \quad (1)$$

where, $P_{m,d}^{cor}$ is corrected GCM rainfall a on the d^{th} day of m^{th} month, and $P_{raw,m}$ is the raw GCM rainfall on the d^{th} day of m^{th} month. μ represents the expectation operator (e.g., μ $P_{obs,m}$ represents the mean value of observed rainfall at given mon^{th} m).

Power transformation method (PT)

The PT is a nonlinear method which corrects both mean and variance of rainfall:

$$P_{cor} = a.P^b \quad (2)$$

where P_{cor} is corrected GCM rainfall, P is raw GCM rainfall, a and b are the parameters obtained during the calibration period.

Gamma quantile mapping (Gamma QM)

The Gamma QM is a distribution mapping method which adjusts the GCM rainfall such that its statistical distribution matches with APHRODITE rainfall. It constructs a transfer function that transforms GCM rainfall to probabilities via the cumulative distribution function (CDF), and then transforms them back into data values using the inverse CDF (or quantile function) of the APHRODITE distribution The Gamma QM is a parametric quantile mapping which uses gamma distribution to represent the probability distribution function of GCM precipitation depending on two parameters. The gamma distribution is defined as:

$$f(x) = \frac{(x/\beta)^{\alpha-1}\exp(-x/\beta)}{\beta\Gamma(x)} x, \alpha, \beta > 0 \quad (3)$$

where, α is the scale parameter, β is the shape parameter and Γ is the gamma function.

Generalized quantile mapping (Gen QM)

The Gen QM is also a parametric quantile mapping but using two theoretical distributions, the gamma distribution

Table 3 | The performance of different bias correction methods

	Mean rainfall		Standard deviation	
Bias correction methodology	**R^2**	**NRMSE (%)**	**R^2**	**NRMSE (%)**
Scaling	0.92	32.2	0.02	104.5
Gamma QM	0.88	37.5	0.67	67.1
PT	**0.98**	**13**	**0.95**	**21.7**
Gen QM	0.33	87	0.02	105.6

The bold values represent the nearest to the optimum for each statistical metric.

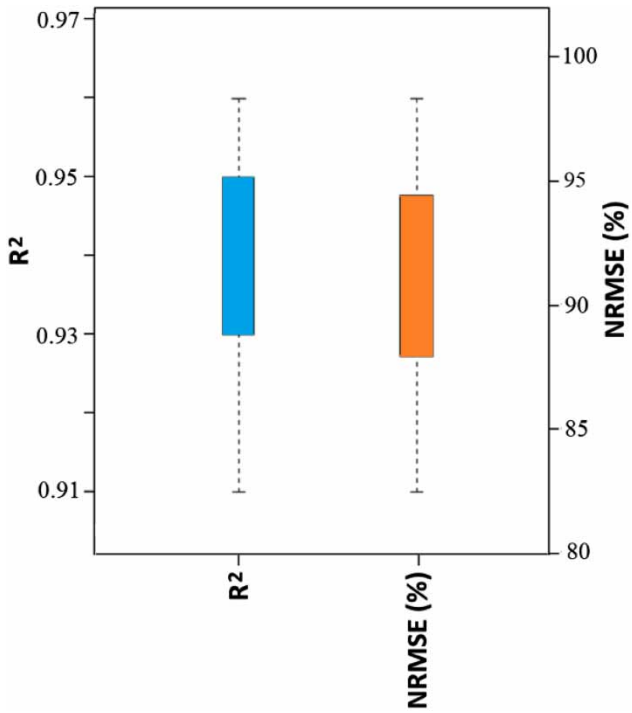

Figure 3 | Box plot of metrics, R^2 and NRMSE used for the evaluation of the performance of the MME model at different grid points over Peninsular Malaysia.

and generalized Pareto distribution (GPD). By default, it applies a gamma distribution to values under the threshold given by the 95th percentile and a general Pareto distribution (GPD) to values above the threshold. The density function of the three-parameter GPD is:

$$f(x) = (1/\sigma)1 + (\xi/\sigma)(x-\mu))^{-1-\frac{-1}{\xi}} \; x \geq \mu, \; \sigma > 0, \; \xi > 0$$

where, σ is the scale parameter, ξ the shape parameter and μ is the location parameter.

Multi-model ensemble (MME) projections

Different GCMs projections have obvious heterogeneity and uncertainties. To reduce the associated uncertainty and improve the accuracy of the projection, the MME was adopted in this study using the downscaled outputs of four GCMs. For this purpose, a nonlinear RF regression technique was applied at all the APHRODITE grid points. The RF is a technique of regression using classification or regression trees (Breiman *et al.* 1984; Breiman 2001). It starts by sampling different bootstrap data to be used to construct each tree. Then, classification and regression tree method were used to develop unpruned trees using each bootstrap sample. The performance of the forest in predicting the new data was assessed by aggregating the predictions of all trees in the forest. This procedure was repeated with new bootstrap samples until all data are used completely. The RF having the least error is considered as the best model. The performance of the final MME was evaluated using R^2 and NRMSE.

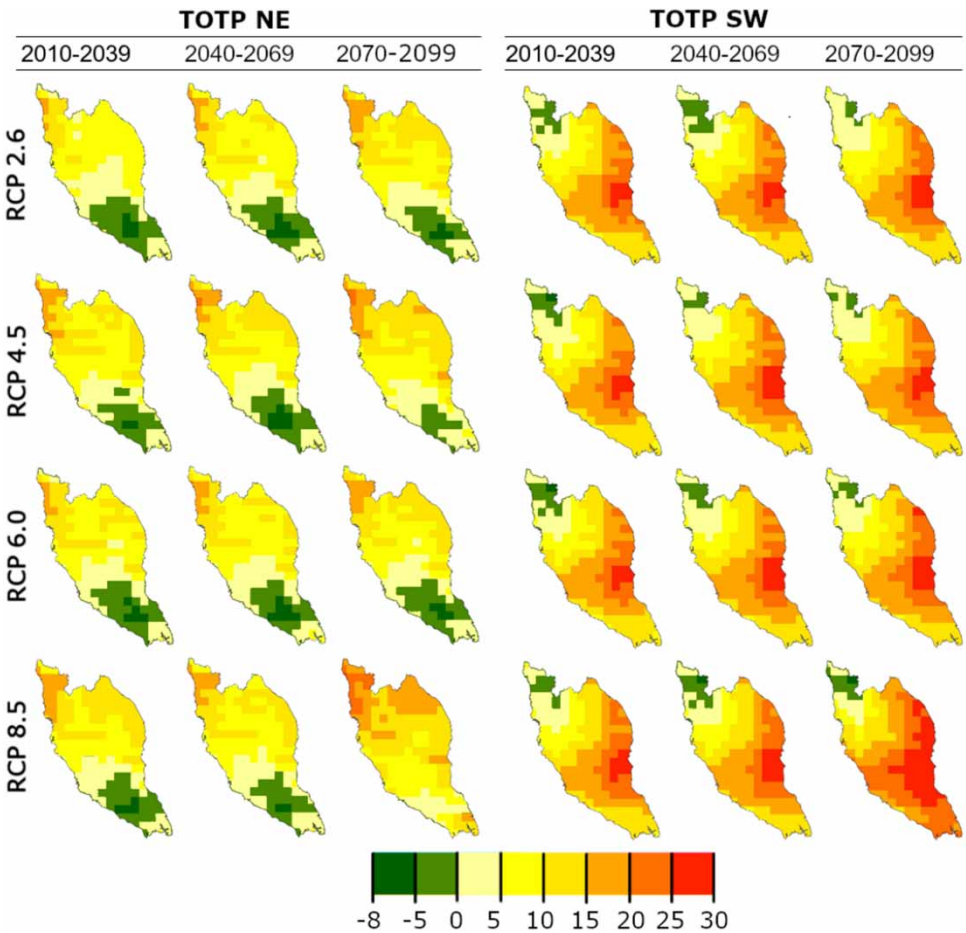

Figure 4 | The percentage of changes in total precipitation in wet days (TOTP) in future periods, 2010–2039, 2040–2069 and 2070–2099 compared to base year (1961–2005) APHRODITE rainfall during northeast and southwest monsoons for different RCP scenarios.

The developed MME model was then used to project future rainfall during the period 2010–2099 for RCP2.6, RCP4.5, RCP6.0 and RCP8.5. The extreme rainfall indices were calculated for three separate future periods (2010–2039, 2040–2069 and 2070–2099) and the spatial and temporal variations were compared with the historical APHRODITE rainfall data to assess their changes.

RESULTS

Evaluation of bias correction methodologies

The bias in the GCM simulated rainfall was corrected using four bias correction methods, namely, scaling, PT, Gen QM and Gamma QM against APHRODITE for the period 1961–2005. The performance of the bias correction methods was evaluated by comparing the monthly climatology of mean rainfall and standard deviation of the bias-corrected outputs with the APHRODITE data. The bias corrected and APHRODITE mean rainfall and standard deviation of the four GCMs are shown in Figure 2. From Figure 2 it can be found that the PT method is performing well compared to other bias correction approaches used. The R^2 and NRMSE in bias-corrected rainfall of each GCM by the four bias correction methods are presented in Table 3. It can be clearly observed from Table 3 that bias-corrected rainfall by PT was the nearest to the optimum R^2 and RMSE. Therefore, PT was selected for the correction of bias in GCM simulated rainfall for both historical and future periods.

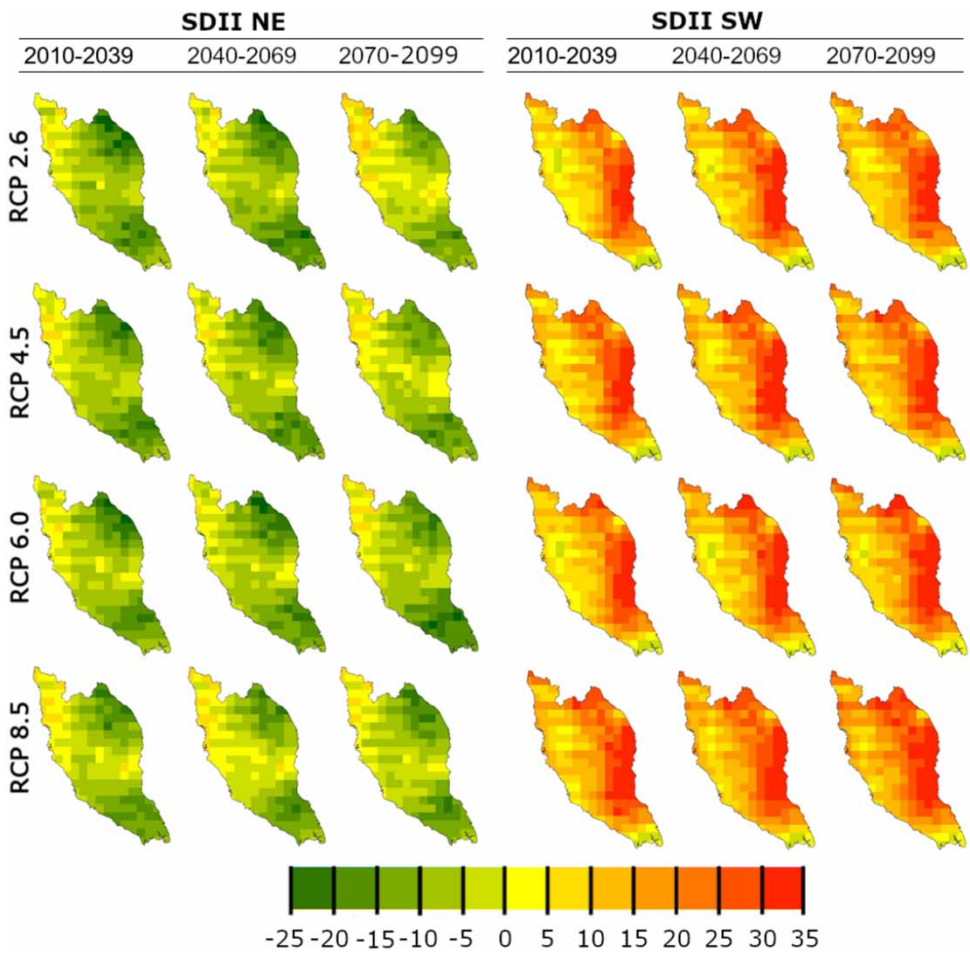

Figure 5 | The percentage of changes in simple daily precipitation intensity (SDII) in the future periods, 2010–2039, 2040–2069 and 2070–2099 compared to base year (1961–2005) APHRODITE rainfall during northeast and southwest monsoons for different RCP scenarios.

The bias correction techniques used in this study of MOS downscaling have their inherent advantages and drawbacks. The scaling method can accurately correct the biases in mean rainfall; however, the biases in variance cannot be removed using this approach. Both mean and variance can be corrected using the PT method, but it cannot correct the probability in wet days. The QM method attempts to correct all the statistical moments such as mean, standard deviation, skewness, kurtosis as well as statistical attributes such as extremes (Fang *et al.* 2015). Different forms of QM, such as generalized QM and Gamma QM have been developed where cumulative distribution functions (CDFs) of GCM simulated historical rainfall and the observed rainfall are equated (Sachindra *et al.* 2014). The major problem of QM methods is that they often disrupt the temporal sequence. Therefore, none of the bias correction methods can be considered good or bad for downscaling rainfall (Maraun *et al.* 2010; Sachindra *et al.* 2014). The appropriate bias correction approach should be selected by comparing the performance of different bias correction techniques.

Performance evaluation of the MME mean rainfall

To assess the spatial and temporal changes in rainfall extremes in Peninsular Malaysia, a single MME mean rainfall was developed from the four GCMs' projected rainfall using RF. The MME mean rainfall was generated for all the four RCPs separately for the period 2010–2099. The performance of the MME model was assessed for the historical period 1961–2005 against APHRODITE rainfall using R^2 and NRMSE. The obtained results for all the

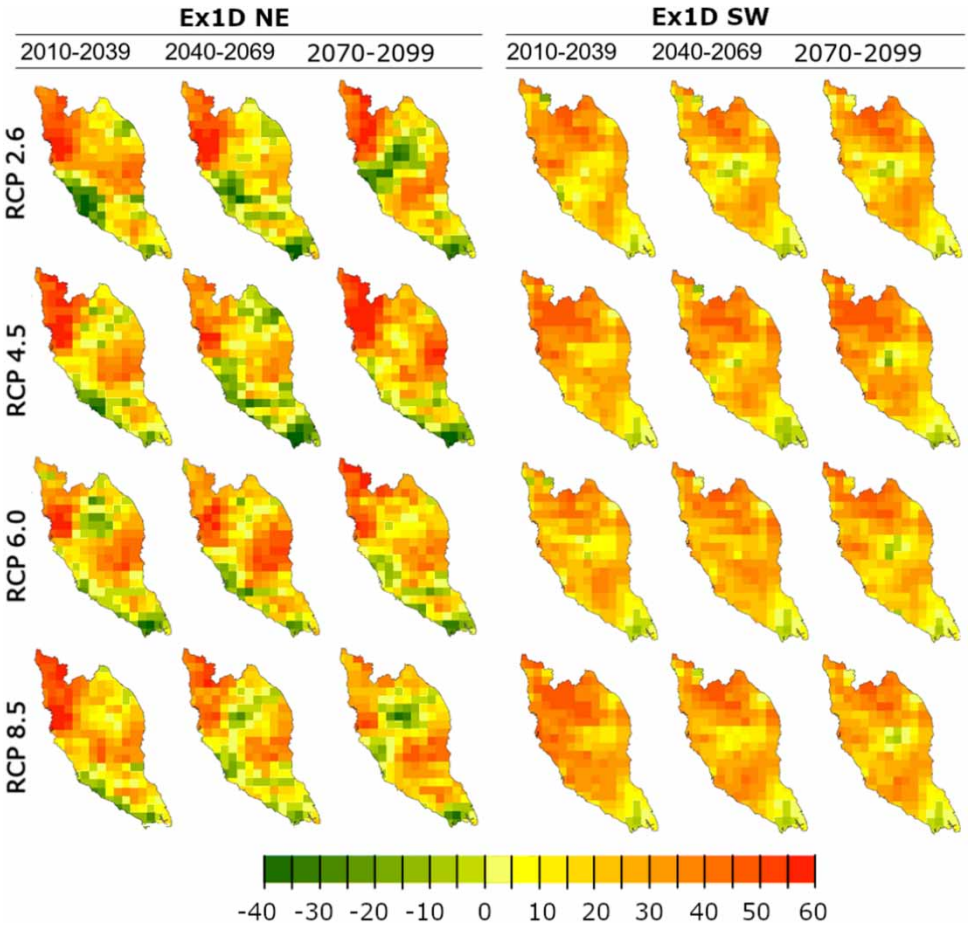

Figure 6 | Percentage of changes in maximum 1-day projected rainfall (Ex1D) in future periods, 2010–2039, 2040–2069 and 2070–2099 compared to base year (1961–2005) APHRODITE rainfall during northeast and southwest monsoons for different RCP scenarios.

grids over the study area are shown in Figure 3. The figure shows high performance of the MME model in terms of both R^2 and NRMSE. It can be noticed that the developed MME is able to reduce the uncertainties associated with the individual GCMs sufficiently and thus able to improve the accuracy of rainfall projection. The projected rainfall of the MME model for the period 2010–2099 under RCP2.6, RCP4.5, RCP6.0 and RCP8.5 was used to assess the changes in rainfall extremes for Peninsular Malaysia.

Changes in projected rainfall extremes

The spatial variation in annual rainfall was computed by comparing the annual MME projected rainfall with APHRODITE gridded rainfall for all the grids over Peninsular Malaysia for three periods, 2010–2039, 2040–2069 and 2070–2099. The spatial distribution of APHRODITE annual rainfall (1961–2005) for Peninsular Malaysia is shown in Figure 1. The spatial changes in rainfall extremes were evaluated using eight extreme indices defined in Table 2. The changes for continuous dry days (CDD), consecutive wet days (CWD), R20 and TRD were estimated in number of days while EX5D, SDII and TOTP were estimated in percentage. The changes were evaluated by comparing the projected extremes for three periods, 2010–2039, 2040–2069 and 2070–2099 with the same extreme indices estimated using APHRODITE rainfall for the period 1961–2005 for all grids of Peninsular Malaysia. The assessment was performed for two seasons, NE monsoon and SW monsoon, for each RCP scenario.

The spatial distribution of the percentage of variation in the total precipitation in wet days (TOTP) during the NE and SW monsoons for four RCPs is presented in Figure 4. Overall, the variation of TOTP was found in the range between −7.37%

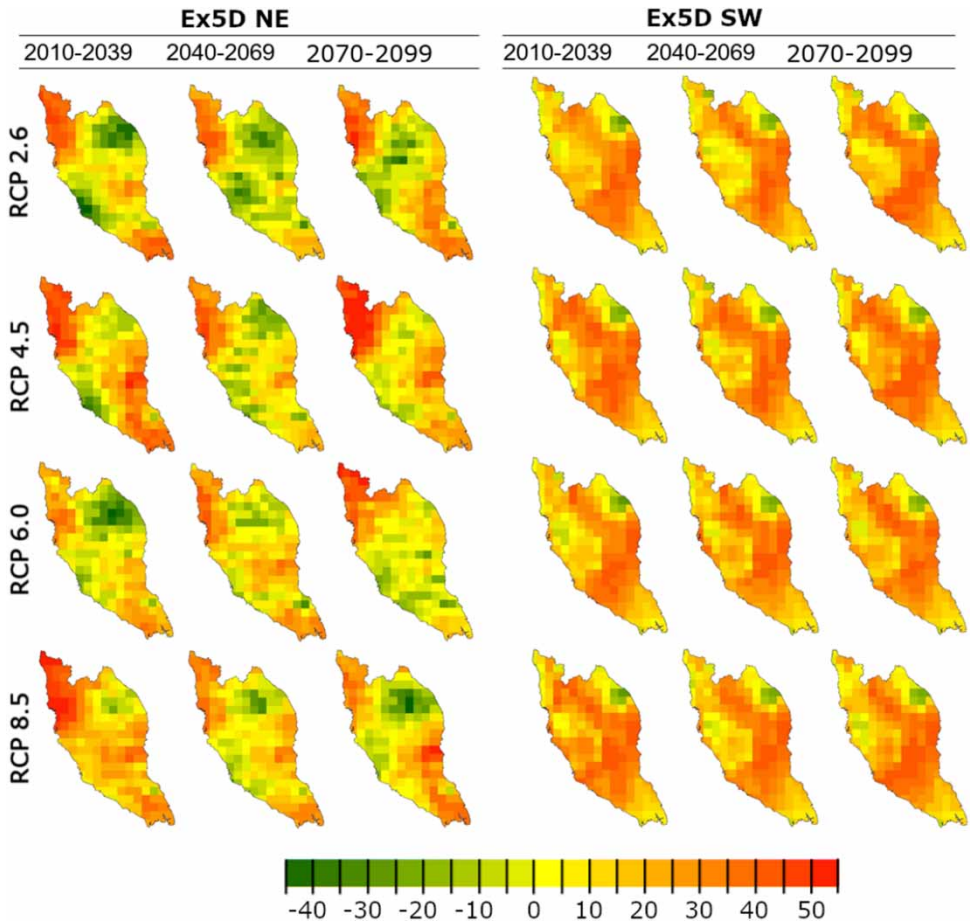

Figure 7 | Percentage of changes in maximum 5-day projected rainfall (Ex5D) in future periods, 2010–2039, 2040–2069 and 2070–2099 compared to base year (1961–2005) APHRODITE rainfall during northeast and southwest monsoons for different RCP scenarios.

and 29.45% during both seasons. However, the increase was projected to be higher during SW monsoon than the NE monsoon. During the NE monsoon, the increase in TOTP was observed in the north of the peninsular for all the RCPs up to 25%, while it was found to increase by 29.45% on the west coast during the SW monsoon. A consistent decrease in TOTP was also observed for all RCPs for all the three future periods in the northwest of the study area during the SW monsoon.

Figure 5 represents the percentage of variation in the spatial distribution of the simple daily precipitation intensity (SDII) during the NE and SW monsoons under the four RCPs. A consistent decrease (increase) in the SDII during the NE (SW) monsoon was observed for four RCPs. During the NE monsoon, the variation was in the range of −25% to 10%. The decrease in the SDII was observed in the northeast and the southwest while the increase was observed mostly in the northwest. During the SW monsoon, the per cent of variation for SDII was in the range of −5% to 35%. An increase in SDII was observed in the entire peninsula except for the southern tip where it was found to decrease by −5%.

Percentage of changes in maximum 1-day rainfall (Ex1D) in three future periods and RCP scenarios are shown in Figure 6. For the NE monsoon, a change in Ex1D in the range of −40% to 60% was observed. For the SW monsoon, the variation was in the range of −15% to 50%. The variation was almost the same for both NE and SW monsoons. An increase in Ex1D was observed in the northern region while a decrease was seen in the south and southwest region.

The percentage of changes in the maximum 5-day rainfall is shown in Figure 7. The observed change was in the range of

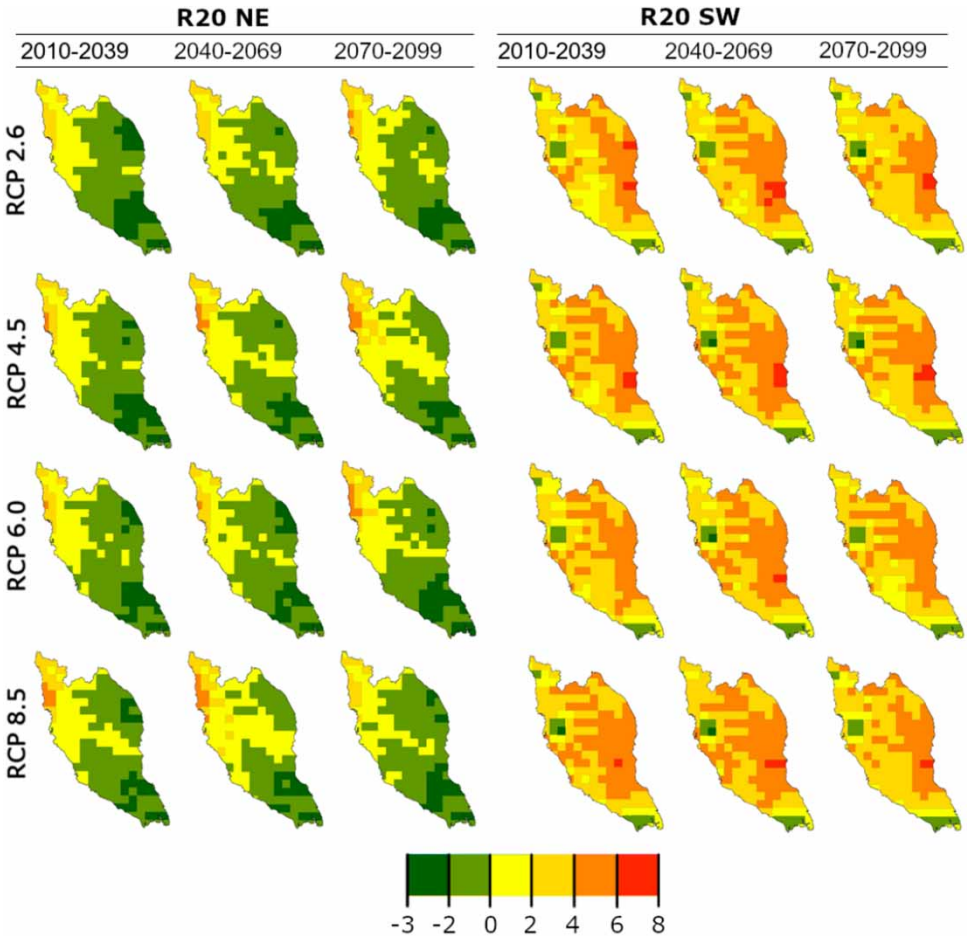

Figure 8 | Variation in number of days with 20 mm rainfall (R20) in future periods, 2010–2039, 2040–2069 and 2070–2099 compared to base year (1961–2005) APHRODITE rainfall during northeast and southwest monsoons for different RCP scenarios.

−45% to 55% during the NE monsoon, while it was in the range of −25% to 45% during the SW monsoon. The variation in spatial distribution of this index was found to be similar for both NE and SW monsoons. The maximum increase was observed in the north with a decrease in the east for both the seasons.

Changes in the number of days with 20 mm rainfall (R20) is shown in Figure 8. A decrease in R20 was observed in most parts of Peninsular Malaysia while there was an increase in the northern region during the NE monsoon. An increase in R20 was observed for the SW monsoon in most parts of the country. However, a decrease was also observed in some parts in the coastal region in the south and west during the SW monsoon.

Figure 9 shows the variation in CDD in Peninsular Malaysia under different RCPs. During the NE monsoon, the number of CDD was found to decrease in the east and increase in the south. For the SW monsoon, the number of CDD was found to decrease in the north, while increasing in the south. It can be noted that there would be more wet days during the SW monsoon as the number of CDD during the SW monsoon are less as compared to the NE monsoon.

Figure 10 shows the changes in the number of CWD for different future periods and scenarios. The number of CWD was found to increase in the southern region while decreasing in the northern region during the NE monsoon. In the SW monsoon, it was found to increase in the north and northeast, but decrease in the south.

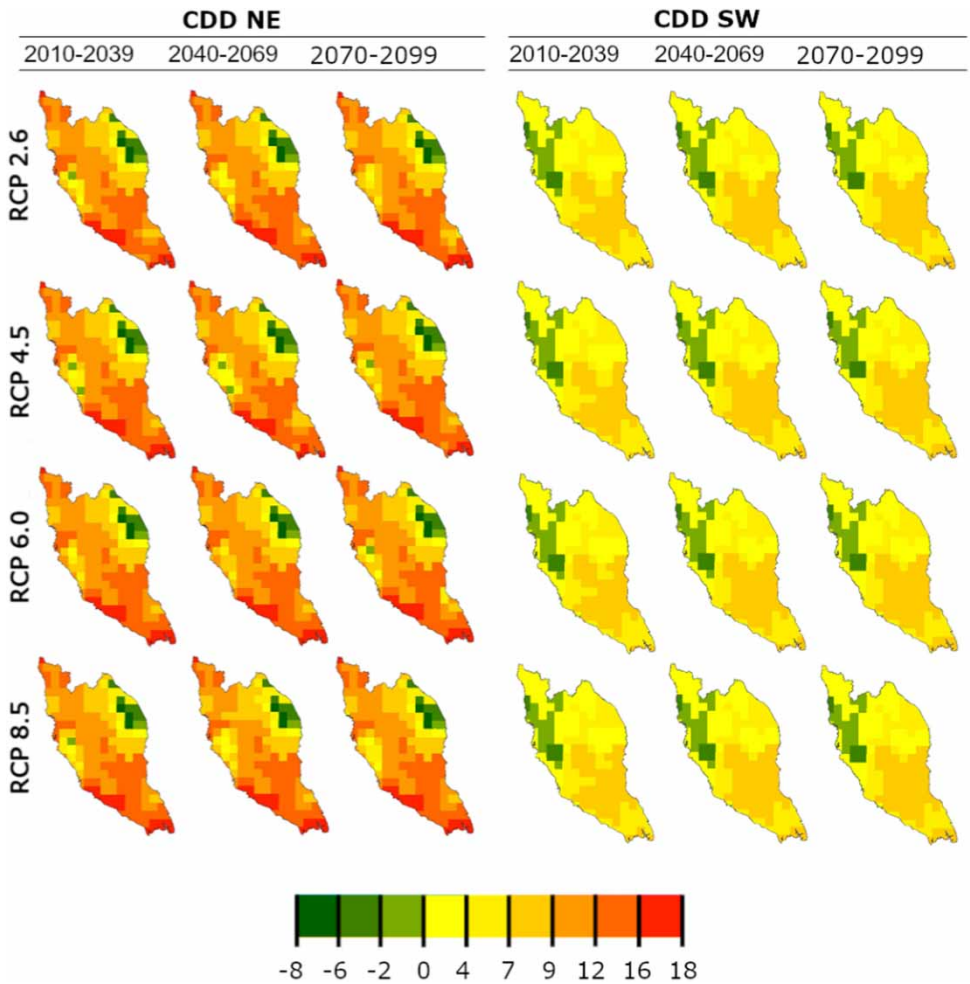

Figure 9 | Changes in the number of consecutive dry days (CDD) in future periods, 2010–2039, 2040–2069 and 2070–2099 compared to base year (1961–2005) APHRODITE rainfall during northeast and southwest monsoons for different RCP scenarios.

Figure 11 illustrates the changes in total number of rainy days (TRD) in a year in Peninsular Malaysia due to climate change. The TRD was found to increase in most parts of the country during both the seasons, although a decrease was also observed in the south. The patterns of spatial distribution were almost the same during both the seasons. However, a higher variation (−30 to +60 days) was observed during the SW monsoon compared to NE monsoon.

DISCUSSION

A MOS-based statistical downscaling approach was used to downscale the rainfall from selected GCMs. For this purpose, four commonly used bias correction approaches were compared and the most suitable downscaling technique was used to project the rainfall. An MME model was developed to generate a single rainfall projection from the simulations of four GCMs in order to project the spatiotemporal changes in rainfall extremes in Peninsular Malaysia. Finally, the spatial variation of MME projected extreme indices was compared with that estimated using APHRODITE rainfall for the historical period to show the possible changes. The PT was found to be the most suitable downscaling method. It was observed that MME can efficiently project the rainfall. Therefore, the MME projected rainfall was used to assess the variations in the annual extremes for Peninsular Malaysia.

During the NE monsoon, the number of CDD was found to decrease in the east and number of CWD was found to increase in the south, which means there will be more rainy days in the south and east during the NE monsoon. During the SW monsoon, the maximum number of CWD was

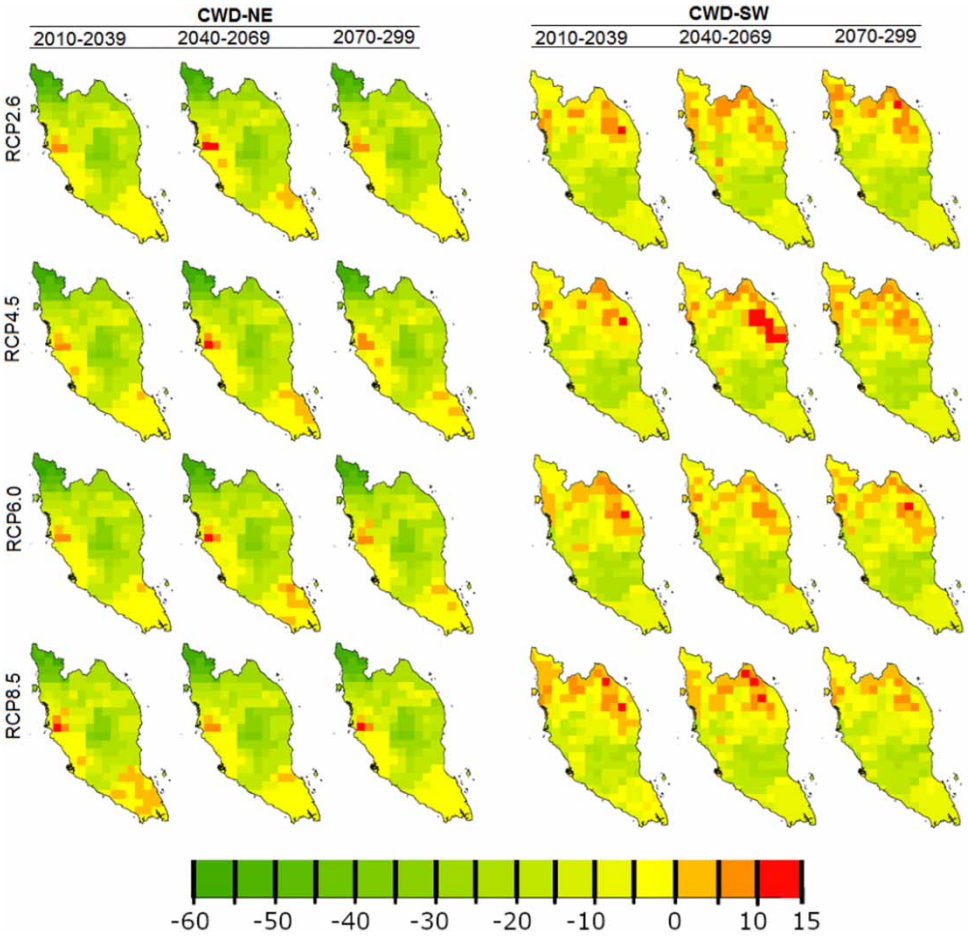

Figure 10 | Projected changes in the number of consecutive wet days (CWD) in future periods, 2010–2039, 2040–2069 and 2070–2099 compared to base year (1961–2005) APHRODITE rainfall during northeast and southwest monsoons for different RCP scenarios.

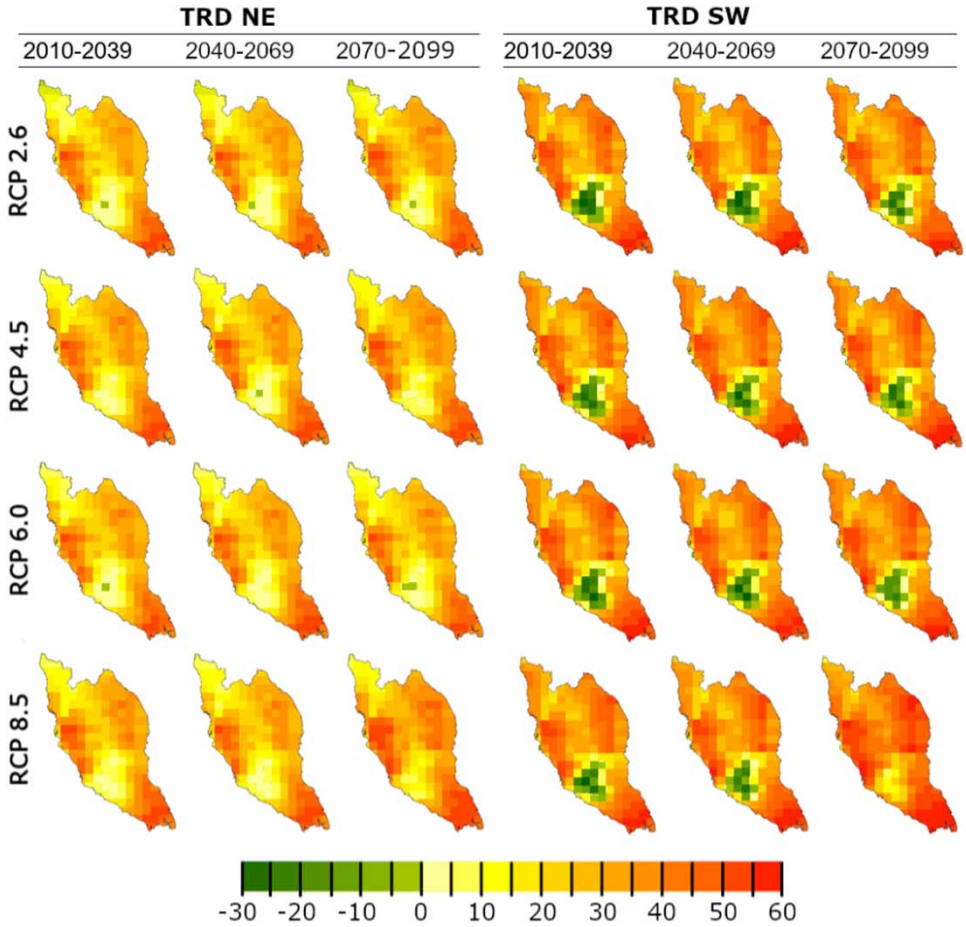

Figure 11 | Projected changes in number of total rainy days (TRD) in future periods, 2010–2039, 2040–2069 and 2070–2099 compared to base year (1961–2005) APHRODITE rainfall during northeast and southwest monsoons for different RCP scenarios.

found to increase in the north and northeast, while a decrease in the number of CDD was found in the north, which means the north can have rainier days during the SW monsoon.

There may be more wet days during the SW monsoon as the number of CDD during SW monsoon are projected to be less compared to the NE monsoon. For maximum 1-day rainfall, the overall changes in both NE and SW monsoons were similar. The overall increase was observed in the northern region. For maximum 5-day rainfall, the changes were also found to be similar for both NE and SW monsoons. The maximum increase was observed in the northern region. It can be said that more and intense rainfall can happen in the northern part due to climate change. The range of change was found greater during the NE monsoon for both maximum 1-day and maximum 5-day rainfall. For R20, the maximum increase was observed in the northern part during the NE monsoon, while the increase was observed in almost all parts of the country during the SW monsoon. In the case of SDII, more variation was observed during the SW monsoon compared to NE monsoon. The increase in TOTP was observed in the east while a decrease was found in the north of the peninsula. The TRD was found to increase in most parts of the country during both the seasons, although a decrease was also observed in the south. The spatial distribution was found to be almost the same during both the seasons; however, more variation in TRD was observed during the SW monsoon compared to NE monsoon.

CONCLUSION

Although both an increase and decrease were observed for different indices, it can be concluded that future seasonal

rainfall will vary for all the periods. The results indicate that both droughts and floods can happen due to changes in climate. During the SW monsoon, there will be more wet days as compared to the NE monsoon. For most of the indices, the maximum change was observed under RCP8.5 and mostly in the last part of this century, except for Ex1D and Ex5D which were found to change more under RCP4.5 for both NE and SW monsoons. The greater variability in rainfall extremes was observed in the northeast region. As compared to other regions, this region is more vulnerable to hydro-climatic disasters. Results indicate that climate change can increase the possibility of hydro-climatic disasters in this part of Peninsular Malaysia.

In this study, we used MOS-based statistical downscaling method; PP method can also be used, and the obtained results can be compared with the MOS method in future. Four GCMs were used to develop a MME for the projection of rainfall extremes, more or less number of other GCMs, chosen using different GCM selection methods, can be developed for using MME. For assessing the changes in rainfall extreme indices, the MME projected rainfall was compared with the APHRODITE rainfall indices. Other types of gridded data products can be used for assessing uncertainty in projection that arises due to the gridded data used.

ACKNOWLEDGEMENT

The authors would like to acknowledge Universiti Teknologi Malaysia (UTM) for providing financial support for this research through RUG Grant No. Q.J130000.2522.18H94.

REFERENCES

Ahmed, K., Shahid, S., Haroon, S. B. & Wang, X.-J. 2015a Multilayer perceptron neural network for downscaling rainfall in arid region: a case study of Baluchistan, Pakistan. *Journal of Earth System Science* **124**, 1325–1341.

Ahmed, K., Shahid, S., Harun, S. & Nawaz, N. 2015b Performance assessment of different bias correction methods in statistical downscaling of precipitation. *Malaysian Journal of Civil Engineering* **27**, 311–324.

Ahmed, K., Shahid, S., Nawaz, N. & Khan, N. 2018 Modeling climate change impacts on precipitation in arid regions of Pakistan: a non-local model output statistics downscaling approach. *Theoretical and Applied Climatology* **137**, 1347–1364.

Ahmed, K., Sachindra, D. A., Shahid, S., Demirel, M. C. & Chung, E.-S. 2019 Selection of multi-model ensemble of GCMs for the simulation of precipitation based on spatial assessment metrics. *Hydrology and Earth System Sciences Discussions*. doi:https://doi.org/10.5194/hess-2018-585.

Alexander, L., Zhang, X., Peterson, T., Caesar, J., Gleason, B., Tank, A. K., Haylock, M., Collins, D., Trewin, B. & Rahimzadeh, F. 2006 Global observed changes in daily climate extremes of temperature and precipitation. *Journal of Geophysical Research: Atmospheres* **111**, 95–114.

Batisani, N. & Yarnal, B. 2010 Rainfall variability and trends in semi-arid Botswana: implications for climate change adaptation policy. *Applied Geography* **30**, 483–489.

Breiman, L. 2001 Random forests. *Machine Learning* **45**, 5–32.

Breiman, L., Friedman, J., Olshen, R. & Stone, C. 1984 *Classification and Regression Trees*, Cole Statistics/ Probability Series. Chapman & Hall, New York, USA.

Chen, A., Chen, D. & Azorin-Molina, C. 2018a Assessing reliability of precipitation data over the Mekong River Basin: a comparison of ground-based, satellite, and reanalysis datasets. *International Journal of Climatology* **38**, 4314–4334.

Chen, J., Li, C., Brissette, F. P., Chen, H., Wang, M. & Essou, G. R. 2018b Impacts of correcting the inter-variable correlation of climate model outputs on hydrological modeling. *Journal of Hydrology* **560**, 326–341.

Chen, J., Brissette, F. P., Zhang, X. J., Chen, H., Guo, S. & Zhao, Y. 2019 Bias correcting climate model multi-member ensembles to assess climate change impacts on hydrology. *Climatic Change* **153**, 361–377.

Donat, M., Alexander, L., Yang, H., Durre, I., Vose, R., Dunn, R., Willett, K., Aguilar, E., Brunet, M. & Caesar, J. 2013 Updated analyses of temperature and precipitation extreme indices since the beginning of the twentieth century: the HadEX2 dataset. *Journal of Geophysical Research: Atmospheres* **118**, 2098–2118.

Eden, J. M. & Widmann, M. 2014 Downscaling of GCM-simulated precipitation using model output statistics. *Journal of Climate* **27**, 312–324.

Fang, G., Yang, J., Chen, Y. & Zammit, C. 2015 Comparing bias correction methods in downscaling meteorological variables for a hydrologic impact study in an arid area in China. *Hydrology and Earth System Sciences* **19**, 2547–2559.

Gleckler, P. J., Taylor, K. E. & Doutriaux, C. 2008 Performance metrics for climate models. *Journal of Geophysical Research: Atmospheres* **113**, D06104.

Gudmundsson, L., Bremnes, J., Haugen, J. & Engen-Skaugen, T. 2012 Technical note: downscaling RCM precipitation to the station scale using statistical transformations–a comparison of methods. *Hydrology and Earth System Sciences* **16**, 3383–3390.

Guo, Q., Chen, J., Zhang, X., Shen, M., Chen, H. & Guo, S. 2019 A new two-stage multivariate quantile mapping method for bias correcting climate model outputs. *Climate Dynamics* **53**, 3603–3623.

Ines, A. V. & Hansen, J. W. 2006 Bias correction of daily GCM rainfall for crop simulation studies. *Agricultural and Forest Meteorology* **138**, 44–53.

IPCC 2013 *Fifth Assessment Report (AR5)*. Intergovernmental Panel on Climate Change.

Ishizaki, N. N., Dairaku, K. & Ueno, G. 2017 Regional probabilistic climate projection for Japan with a regression model using multi-model ensemble experiments. *Hydrological Research Letters* **11**, 44–50.

Jiang, Z., Song, J., Li, L., Chen, W., Wang, Z. & Wang, J. 2012 Extreme climate events in China: IPCC-AR4 model evaluation and projection. *Climatic Change* **110**, 385–401.

Khan, N., Shahid, S., Ahmed, K., Ismail, T., Nawaz, N. & Son, M. 2018 Performance assessment of general circulation model in simulating daily precipitation and temperature using multiple gridded datasets. *Water* **10**, 1793.

Khan, N., Pour, S. H., Shahid, S., Ismail, T., Ahmed, K., Chung, E. S., Nawaz, N. & Wang, X. 2019 Spatial distribution of secular trends in rainfall indices of Peninsular Malaysia in the presence of long-term persistence. *Meteorological Applications* **26**, 655–670.

Li, H., Sheffield, J. & Wood, E. F. 2010 Bias correction of monthly precipitation and temperature fields from intergovernmental panel on climate change AR4 models using equidistant quantile matching. *Journal of Geophysical Research: Atmospheres* **115**, D10101. doi:10.1029/2009JD012882.

Lin, G.-F., Chang, M.-J. & Wu, J.-T. 2017 A hybrid statistical downscaling method based on the classification of rainfall patterns. *Water Resources Management* **31**, 377–401.

Lutz, A. F., ter Maat, H. W., Biemans, H., Shrestha, A. B., Wester, P. & Immerzeel, W. W. 2016 Selecting representative climate models for climate change impact studies: an advanced envelope-based selection approach. *International Journal of Climatology* **36**, 3988–4005.

Maraun, D., Wetterhall, F., Ireson, A., Chandler, R., Kendon, E., Widmann, M., Brienen, S., Rust, H., Sauter, T. & Themeßl, M. 2010 Precipitation downscaling under climate change: recent developments to bridge the gap between dynamical models and the end user. *Reviews of Geophysics* **48**, RG3003.

Mayowa, O. O., Pour, S. H., Shahid, S., Mohsenipour, M., Harun, S. B., Heryansyah, A. & Ismail, T. 2015 Trends in rainfall and rainfall-related extremes in the east coast of peninsular Malaysia. *Journal of Earth System Science* **124**, 1609–1622.

Min, S.-K., Zhang, X., Zwiers, F. W. & Hegerl, G. C. 2011 Human contribution to more-intense precipitation extremes. *Nature* **470**, 378.

Mpelasoka, F. S. & Chiew, F. H. 2009 Influence of rainfall scenario construction methods on runoff projections. *Journal of Hydrometeorology* **10**, 1168–1183.

Muhammad, M. K. I., Nashwan, M. S., Shahid, S., Ismail, T., Song, Y. H. & Chung, E.-S. 2019 Evaluation of empirical reference evapotranspiration models using compromise programming: a case study of Peninsular Malaysia. *Sustainability* **11**, 4267. doi:10.3390/su11164267.

Nashwan, M. S. & Shahid, S. 2019a Spatial distribution of unidirectional trends in climate and weather extremes in Nile river basin. *Theoretical and Applied Climatology* **137**, 1181–1199. doi:10.1007/s00704-018-2664-5.

Nashwan, M. S. & Shahid, S. 2019b Symmetrical uncertainty and random forest for the evaluation of gridded precipitation and temperature data, *Atmospheric Research* **230**, 104632. doi:10.1016/j.atmosres.2019.104632.

Nashwan, M. S., Ismail, T. & Ahmed, K. 2018a Flood susceptibility assessment in Kelantan river basin using copula. *International Journal of Engineering and Technology* **7**, 584–590. doi:10.14419/ijet.v7i2.10447.

Nashwan, M. S., Shahid, S., Chung, E.-S., Ahmed, K. & Song, Y. H. 2018b Development of climate-based index for hydrologic hazard susceptibility. *Sustainability* **10**, 2182. doi:10.3390/su10072182.

Nashwan, M. S., Ismail, T. & Ahmed, K. 2019a Non-stationary analysis of extreme rainfall in Peninsular Malaysia. *Journal of Sustainability Science and Management* **14**, 17–34.

Nashwan, M. S., Shahid, S. & Abd Rahim, N. 2019b Unidirectional trends in annual and seasonal climate and extremes in Egypt. *Theoretical and Applied Climatology* **136**, 457–473. doi:10.1007/s00704-018-2498-1.

Nashwan, M. S., Shahid, S. & Wang, X.-j. 2019c Assessment of satellite-based precipitation measurement products over the hot desert climate of Egypt. *Remote Sensing* **11**, 555. doi:10.3390/rs11050555.

Nashwan, M. S., Shahid, S. & Wang, X.-j. 2019d Uncertainty in estimated trends using gridded rainfall data: a case study of Bangladesh. *Water* **11**, 349. doi:10.3390/w11020349.

Noor, M., Ismail, T., Chung, E.-S., Shahid, S. & Sung, J. 2018 Uncertainty in rainfall intensity duration frequency curves of Peninsular Malaysia under changing climate scenarios. *Water* **10**, 1750.

Noor, M., bin Ismail, T., Shahid, S., Ahmed, K., Chung, E.-S. & Nawaz, N. 2019 Selection of CMIP5 multi-model ensemble for the projection of spatial and temporal variability of rainfall in peninsular Malaysia. *Theoretical and Applied Climatology* **138**, 999–1012.

Ou, T., Chen, D., Linderholm, H. W. & Jeong, J.-H. 2013 Evaluation of global climate models in simulating extreme precipitation in China. *Tellus A: Dynamic Meteorology and Oceanography* **65**, 19799.

Paterson, R. R. M., Kumar, L., Taylor, S. & Lima, N. 2015 Future climate effects on suitability for growth of oil palms in Malaysia and Indonesia. *Scientific Reports* **5**, 14457.

Pierce, D. W., Barnett, T. P., Santer, B. D. & Gleckler, P. J. 2009 Selecting global climate models for regional climate change studies. *Proceedings of the National Academy of Sciences of the United States of America* **106**, 8441–8446.

Pour, S. H., Harun, S. B. & Shahid, S. 2014 Genetic programming for the downscaling of extreme rainfall events on the East Coast of Peninsular Malaysia. *Atmosphere* **5**, 914–936. doi:10.3390/atmos5040914.

Pour, S. H., Shahid, S., Chung, E.-S. & Wang, X.-J. 2018 Model output statistics downscaling using support vector machine for the projection of spatial and temporal changes in rainfall of Bangladesh. *Atmospheric Research* **213**, 149–162.

Reichler, T. & Kim, J. 2008 How well do coupled models simulate today's climate? *Bulletin of the American Meteorological Society* **89**, 303–312.

Rupp, D. E., Abatzoglou, J. T., Hegewisch, K. C. & Mote, P. W. 2013 Evaluation of CMIP5 20th century climate simulations for the Pacific Northwest USA. *Journal of Geophysical Research: Atmospheres* **118**, 10884–10906.

Sa'adi, Z., Shahid, S., Chung, E.-S. & bin Ismail, T. 2017 Projection of spatial and temporal changes of rainfall in Sarawak of Borneo Island using statistical downscaling of CMIP5 models. *Atmospheric Research* **197**, 446–460.

Sachindra, D., Huang, F., Barton, A. & Perera, B. 2014 Statistical downscaling of general circulation model outputs to precipitation – part 2: bias-correction and future projections. *International Journal of Climatology* **34**, 3282–3303.

Salman, S. A., Shahid, S., Ismail, T., Ahmed, K. & Wang, X.-J. 2018 Selection of climate models for projection of spatiotemporal changes in temperature of Iraq with uncertainties. *Atmospheric Research* **213**, 509–522.

Scherer, M. & Diffenbaugh, N. S. 2014 Transient twenty-first century changes in daily-scale temperature extremes in the United States. *Climate Dynamics* **42**, 1383–1404.

Shahid, S. 2009 Spatio-temporal variability of rainfall over Bangladesh during the time period 1969–2003. *Asia-Pacific Journal of Atmospheric Science* **45**, 375–389.

Shahid, S. 2010 Rainfall variability and the trends of wet and dry periods in Bangladesh. *International Journal of Climatology* **30**, 2299–2313.

Shahid, S., Wang, X.-J., Harun, S. B., Shamsudin, S. B., Ismail, T. & Minhans, A. 2016 Climate variability and changes in the major cities of Bangladesh: observations, possible impacts and adaptation. *Regional Environmental Change* **16**, 459–471.

Shahid, S., Pour, S. H., Wang, X., Shourav, S. A., Minhans, A. & Ismail, T. 2017 Impacts and adaptation to climate change in Malaysian real estate. *International Journal of Climate Change Strategies and Management* **9**, 87–103.

Sharma, D., Gupta, A. D. & Babel, M. 2007 Spatial disaggregation of bias-corrected GCM precipitation for improved hydrologic simulation: Ping River Basin, Thailand. *Hydrology and Earth System Sciences Discussions* **11**, 1373–1390.

Shiru, M. S., Shahid, S., Chung, E-S. & Alias, N. 2019 Changing characteristics of meteorological droughts in Nigeria during 1901–2010. *Atmospheric Research* **223**, 60–73. doi:10.1016/j.atmosres.2019.03.010.

Sillmann, J., Kharin, V., Zhang, X., Zwiers, F. & Bronaugh, D. 2013a Climate extremes indices in the CMIP5 multimodel ensemble: part 1. Model evaluation in the present climate. *Journal of Geophysical Research: Atmospheres* **118**, 1716–1733.

Sillmann, J., Kharin, V., Zwiers, F., Zhang, X. & Bronaugh, D. 2013b Climate extremes indices in the CMIP5 multimodel ensemble: part 2. Future climate projections. *Journal of Geophysical Research: Atmospheres* **118**, 2473–2493. doi:10.1002/jgrd.50188.

Steinschneider, S., McCrary, R., Mearns, L. O. & Brown, C. 2015 The effects of climate model similarity on probabilistic climate projections and the implications for local, risk-based adaptation planning. *Geophysical Research Letters* **42**, 5014–5044.

Turco, M., Llasat, M. C., Herrera, S. & Gutiérrez, J. M. 2017 Bias correction and downscaling of future RCM precipitation projections using a MOS-Analog technique. *Journal of Geophysical Research: Atmospheres* **122**, 2631–2648.

Wang, X.-j., Zhang, J.-y., Wang, J.-h., He, R.-min., Amgad, E., Liu, J.-h., Wang, X.-g., David, K. & Shahid, S. 2014 Climate change and water resources management in Tuwei river basin of Northwest China. *Mitigation and Adaptation Strategies for Global Change* **19**, 107–120.

Wang, X.-j., Zhang, J.-y., Shamsuddin, S., Oyang, R.-l., Guan, T.-s., Xue, J.-g. & Zhang, X. 2017 Impacts of climate variability and changes on domestic water use in the Yellow River Basin of China. *Mitigation and Adaptation Strategies for Global Change* **22**, 595–608.

Wen, Q. H., Zhang, X., Xu, Y. & Wang, B. 2013 Detecting human influence on extreme temperatures in China. *Geophysical Research Letters* **40**, 1171–1176.

Widmann, M., Bretherton, C. S. & Salathé Jr, E. P.. 2003 Statistical precipitation downscaling over the northwestern United States using numerically simulated precipitation as a predictor. *Journal of Climate* **16**, 799–816.

You, Q., Jiang, Z., Wang, D., Pepin, N. & Kang, S. 2018 Simulation of temperature extremes in the Tibetan Plateau from CMIP5 models and comparison with gridded observations. *Climate Dynamics* **51**, 355–369.

Zhang, L. & Yang, X. 2018 Applying a multi-model ensemble method for long-term runoff prediction under climate change scenarios for the Yellow River Basin, China. *Water* **10**, 301.

Zhang, X., Alexander, L., Hegerl, G. C., Jones, P., Tank, A. K., Peterson, T. C., Trewin, B. & Zwiers, F. W. 2011 Indices for monitoring changes in extremes based on daily temperature and precipitation data. *WIREs Climate Change* **2**, 851–870.

Zhou, B., Wen, Q. H., Xu, Y., Song, L. & Zhang, X. 2014 Projected changes in temperature and precipitation extremes in China by the CMIP5 multimodel ensembles. *Journal of Climate* **27**, 6591–6611.

First received 27 June 2019; accepted in revised form 18 September 2019. Available online 5 November 2019